

## Coulomb barriers in the dissociation of doubly charged clusters

F. Garcias\*

*Institut des Sciences Nucléaires, 53 avenue des Martyrs, F-38026 Grenoble, France*

J. A. Alonso and J. M. López

*Departamento de Física Teórica y Física Atómica, Molecular y Nuclear,  
Universidad de Valladolid, E-47071 Valladolid, Spain*

M. Barranco

*Departament d'Estructura i Constituents de la Materia, Facultat de Física, Universitat de Barcelona,  
E-08028 Barcelona, Spain*

(Received 18 September 1990; revised manuscript received 27 November 1990)

The barrier height for the most asymmetric fission decay of doubly charged sodium clusters ( $\text{Na}_N^{2+}$ ) into singly ionized fragments has been computed with use of density-functional theory and the jellium model. We have found that the barrier is sizable for large or intermediate-size clusters, but vanishes for  $N \leq 9$ . We have also computed the energy  $\Delta H_e$  needed to evaporate a neutral monomer from  $\text{Na}_N^{2+}$ . For  $N \leq 40$ , the barrier height is smaller than  $\Delta H_e$ , and emission of a  $\text{Na}^+$  ion is the preferred decay channel of hot  $\text{Na}_N^{2+}$  clusters. On the other hand, the barrier height is larger than  $\Delta H_e$  for  $N > 40$  and, in this case, monomer evaporation becomes competitive. The critical cluster size,  $N_c = 40$ , for the transition from one decay mode to the other is in reasonable agreement with the experimental result. Our calculations suggest that the mechanism for neutral-monomer evaporation is different from the one currently assumed.

### I. INTRODUCTION

Multiply charged clusters  $X_N^{q+}$  are usually observable only beyond a certain critical size  $N_c(q)$  which depends on the charge  $q$ .<sup>1</sup> It is commonly admitted that the critical size can be interpreted as the size below which the Coulomb repulsion between the positive holes makes the cluster unstable against fragmentation into clusters with smaller charges. A purely energetic criterion has been proposed by several authors.<sup>2-4</sup> According to this criterion,  $N_c(q)$  is the size below which the sum of the ground-state energies of the fragments is lower than the ground-state energy of the parent cluster. The measured critical size is, however, often different for different experiments on clusters of a common element. This fact casts some doubts on a purely energetic criterion. Furthermore, unexpectedly small multiply charged clusters have sometimes been observed,<sup>1,5-8</sup> suggesting that some of these clusters may be metastable, stabilized against fission by large barriers. Explicit calculations for doubly charged transition-metal dimers<sup>9</sup> support this interpretation. Several dimers, such as  $\text{V}_2^{2+}$ ,  $\text{Cr}_2^{2+}$ ,  $\text{Fe}_2^{2+}$ ,  $\text{Nb}_2^{2+}$ ,  $\text{Mo}_2^{2+}$ ,  $\text{Ta}_2^{2+}$ ,  $\text{W}_2^{2+}$ ,  $\text{Rh}_2^{2+}$ , and  $\text{Ir}_2^{2+}$ , were found to be metastable, although stabilized by large barriers. Some others, such as  $\text{Ni}_2^{2+}$ ,  $\text{Co}_2^{2+}$ ,  $\text{Pd}_2^{2+}$ , and  $\text{Pt}_2^{2+}$ , are simply unstable.

Recent experimental work by Bréchnignac *et al.*<sup>10,11</sup> on the induced dissociation of mass-selected doubly charged alkali clusters has clarified substantially some points related to the observability of multiply charged clusters. These authors have noticed that the critical size below

which multiply charged clusters are not observable in mass spectra depends on the cluster-formation mechanism. First of all, one of their key results is that an "excited"  $\text{Na}_N^{2+}$  (or  $\text{K}_N^{2+}$ ) cluster with large  $N$  preferentially evaporates a neutral atom and not a charged fragment  $\text{Na}_p^+$  ( $p < N$ ). The explanation that they propose is that in this size range the fission barrier is larger than the binding energy of the neutral monomer. This means that when  $\text{Na}_N^{2+}$  clusters are formed by atom evaporation from hot clusters of higher masses, the critical size  $N_c$  is the size below which the fission barrier becomes lower than the binding energy of the neutral monomer. However, the same authors also point out that doubly charged clusters can also be formed from cold neutral clusters by a two-step ionization. If the ionization process is such that the cluster is maintained cold, with an internal excitation energy below the top of the Coulomb barrier, metastable doubly charged clusters can exist below the critical size defined above. Stressing the importance of the Coulomb barrier is then a key point of the work of Bréchnignac *et al.* Density-functional calculations for small ( $N = 2-7$ ) charged Mg clusters performed by Reuse *et al.*<sup>12</sup> verify the expectations of Bréchnignac and collaborators. Small  $\text{Mg}_N^{2+}$  clusters are predicted to be metastable, protected against Coulomb dissociation by barriers of a height of 0.5–1 eV. Reuse *et al.* thus conclude that these clusters should be observable.

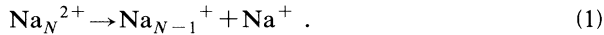
Recently, Saunders<sup>13</sup> has studied the fission behavior of doubly charged Au clusters. The clusters were produced by the liquid-metal ion-source (LMIS) technique, and

$\text{Au}_N^{2+}$  was observed for  $N \geq 9$  (in addition to  $\text{Au}_3^{2+}$ ). The clusters were then fragmented by collisions with Kr atoms. The analysis of the fragmentation products revealed, in agreement with the results of Bréchnignac *et al.*, the competition between neutral-atom evaporation and fission (i.e., decay into two charged fragments). Atom evaporation is dominant for large clusters but fission competes for  $N \leq 18$  and increases strongly as  $N$  decreases. For instance, the fissionability, given by the ratio of the fission and evaporation rates  $\Gamma_f/\Gamma_e$ , increases by four orders of magnitude for  $N$ -even clusters between  $N=18$  and  $N=12$ , having a value of 20–30 for  $N=12$  ( $\Gamma_f/\Gamma_e$  is lower for  $N$ -odd than for  $N$ -even clusters because of a reduced stability of clusters with an odd number of electrons<sup>14</sup>). Saunders finds that the experimental data on the fissionability are consistent with a liquid-drop model similar to the nuclear liquid-drop model.<sup>15</sup> According to this model, the fission barrier becomes zero for  $N < 6$ . This means that  $\text{Au}_N^{2+}$  clusters with  $N < 6$  are predicted to be unstable against spontaneous fission. This critical number is in semiquantitative agreement with the  $N_c = 9$  observed in the LMIS experiments.

It is clear from the work of Bréchnignac *et al.* and of Saunders that a better knowledge of the fission barrier in multiply charged clusters of monovalent (alkali and noble) metals should provide a useful piece of information in the analysis of experiments concerning these clusters. With this motivation in mind, we have undertaken a semiclassical calculation of the fission barrier of doubly charged sodium clusters. This calculation is presented in Sec. II. For this purpose we have used density-functional theory<sup>16</sup> and the jellium model of simple metal clusters.<sup>17</sup> The calculated barrier is then compared to classical estimates. In Sec. III we discuss our results in relation to experiment. Finally, Sec. IV contains a summary.

## II. MODEL FOR CLUSTER DISSOCIATION

In this section we want, first of all, to set up a model for the calculation of the Coulomb barrier and the heat of reaction of the completely asymmetric fission of a doubly charged sodium cluster,

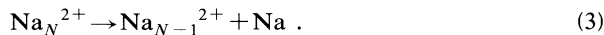


The heat of the reaction is defined in terms of the total ground-state energies of parent and fragments (at infinite separation):

$$\Delta H_f = E(\text{Na}_{N-1}^+) + E(\text{Na}^+) - E(\text{Na}_N^{2+}) . \quad (2)$$

$\Delta H_f$  is negative for small  $N$  and positive for large  $N$ .<sup>4</sup> A negative value of  $\Delta H_f$  means that the reaction is exothermic. On the other hand, the calculation of the fission barrier requires modeling the process by which the ion  $\text{Na}^+$  leaves the remaining fragment.

In a second step we want to compare the probability for reaction (1) with that for the evaporation of a neutral monomer:



The evaporation of a neutral monomer is endothermic—

that is, the heat  $\Delta H_e$  of the reaction is positive:

$$\Delta H_e = E(\text{Na}_{N-1}^{2+}) + E(\text{Na}) - E(\text{Na}_N^{2+}) > 0 . \quad (4)$$

This means that neutral-monomer evaporation cannot occur spontaneously if  $\text{Na}_N^{2+}$  is in its ground state, but it is possible for a highly excited parent cluster. Which of the two reactions (evaporation or fission) occurs depends, as proposed by Bréchnignac *et al.*,<sup>11</sup> on the relative magnitudes of  $\Delta H_e$  and the fission barrier. A schematic representation of this competition is shown in Fig. 1, where the fission barrier is shown along the dissociation coordinate  $d$  (to be defined precisely below). The energy of the system formed by the two ionized fragments ( $\text{Na}_{N-1}^+$  and  $\text{Na}^+$ ) at infinite separation is taken as zero of energies.  $B(d)$  is the barrier for the opposite process of forming  $\text{Na}_N^{2+}$  from  $\text{Na}_{N-1}^+$  and  $\text{Na}^+$ , and  $B_m$  is the maximum of  $B(d)$ . We can call  $B(d)$  the capture barrier and, although the present paper is concerned with fission, we often find it convenient to think in terms of  $B(d)$ . The fission barrier—that is, the barrier for the emission of  $\text{Na}^+$  from  $\text{Na}_N^{2+}$ —is given by

$$F(d) = B(d) + \Delta H_f , \quad (5)$$

and the height of the fission barrier is  $F_m = B_m + \Delta H_f$ . The quantity  $B_m$  is positive.  $F_m$  is larger than  $B_m$  when  $\Delta H_f$  is positive, and smaller than  $B_m$  when  $\Delta H_f$  is negative. According to Bréchnignac *et al.*,<sup>11</sup> evaporation becomes preferred over fission when the condition

$$\Delta H_e < F_m \quad (6)$$

holds.  $\Delta H_e$ ,  $\Delta H_f$ , and  $F(d)$  will now be calculated using an extended Thomas-Fermi approximation.

### A. Jellium model for spherical clusters and heats of reaction

Let us begin with the calculation of  $\Delta H_f$  and  $\Delta H_e$ . These two quantities are defined in Eqs. (2) and (4), respectively. The energies of the clusters involved in these equations are obtained using the spherical-jellium model. This model<sup>4,17</sup> assumes a background of positive charge (representing the ions) with spherical shape and constant density and a distribution of interacting valence electrons (one per atom in the case of Na clusters) with a density  $n(\mathbf{r})$  which is self-consistently calculated in the external potential provided by the positive background. The jellium radius  $R$  is related to the number  $N$  of atoms by  $R = N^{1/3} r_s$ , where  $r_s = 4.0$  is the Wigner-Seitz radius of metallic sodium. Notice that  $R$  remains unchanged when the cluster is ionized.

The ground-state electron density is obtained by minimization of the following extended-Thomas-Fermi (ETF) functional<sup>4,16</sup> (we shall use Hartree atomic units throughout):

$$E[n] = \int \varepsilon[n] d^3r = T + U_{ee} + U_{Je} + U_{JJ} + E_{xc} . \quad (7)$$

$T$  is the electron kinetic energy,<sup>16</sup> given as a sum of the local Thomas-Fermi term and the von Weizsäcker correction ( $\lambda = 1$ ):

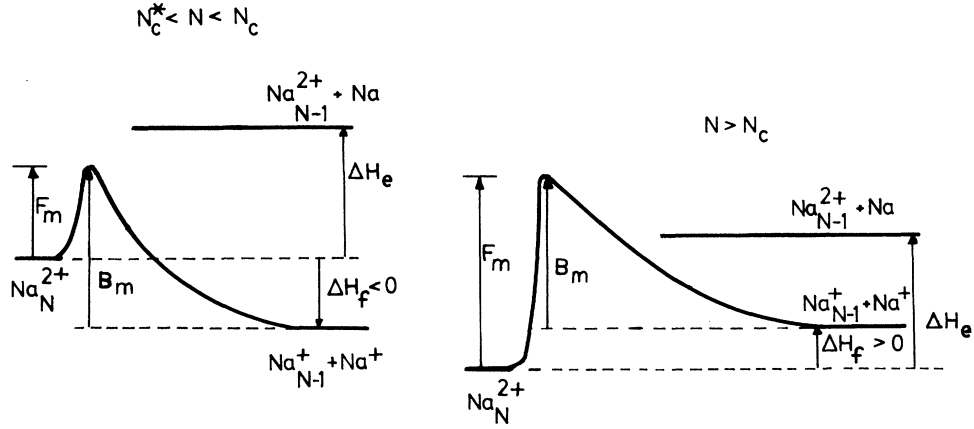


FIG. 1. Schematic representation of the competition between the fission and evaporation reactions. The heats of fission and evaporation are  $\Delta H_f$  and  $\Delta H_e$ , respectively. The capture barrier for the reaction  $\text{Na}_{N-1}^+ + \text{Na}^+ \rightarrow \text{Na}_N^{2+}$  is  $B(d)$ , and the fission barrier is  $F(d) = B(d) + \Delta H_f$ . The maximum values of these two barriers are indicated as  $B_m$  and  $F_m$ , respectively. The fission barrier is lower than the heat of the evaporation in the left panel and larger in the right panel.

$$T[n] = \int d^3r \left[ \frac{3}{10} (3\pi^2)^{2/3} [n(\mathbf{r})]^{5/3} + \frac{\lambda}{8} \frac{[\nabla n(\mathbf{r})]^2}{n(\mathbf{r})} \right]; \quad (8)$$

$U_{ee}$  is the classical Coulomb energy of the electrons,

$$U_{ee} = \frac{1}{2} \int d^3r \int d^3r' \frac{n(\mathbf{r})n(\mathbf{r}')}{|\mathbf{r}-\mathbf{r}'|}; \quad (9)$$

$U_{Je}$  gives the electron-jellium electrostatic interaction,

$$U_{Je} = \int d^3r V_J(\mathbf{r})n(\mathbf{r}); \quad (10)$$

$V_J(\mathbf{r})$  being the jellium potential; and  $U_{JJ}$  is the jellium Coulombic self-interaction. Finally,  $E_{xc}$  is the sum of the electronic exchange and correlation energies. In the local-density approximation (LDA),

$$E_{xc}^{\text{LDA}}[n] = -\frac{3}{4} \left[ \frac{3}{\pi} \right]^{1/3} \int [n(\mathbf{r})]^{4/3} d^3r - \int \frac{0.44n(\mathbf{r})}{7.8 + \left[ \frac{3}{4\pi n(\mathbf{r})} \right]^{1/3}} d^3r, \quad (11)$$

where the first term is the exchange part and the second term uses Wigner's interpolation formula for the correlation energy.<sup>18</sup>

The variational electron density is obtained by solving the Euler-Lagrange equation associated with the functional (7):

$$\frac{\delta E[n]}{\delta n(\mathbf{r})} = \mu, \quad (12)$$

where  $\mu$  is the electron chemical potential. In the case of the spherical-jellium cluster model, Eq. (12) reduces to a one-dimensional radial equation. This case has been discussed in detail previously<sup>4,19</sup> (see also Sec. II B below).  $\Delta H_f$  and  $\Delta H_e$ , which are the heats of the reactions (1) and (3), respectively, are easily obtained since in their calculation one only deals with spherical clusters.

## B. Fission barrier

The simplest model for the barrier  $F(d)$  opposing the dissociation of  $\text{Na}_N^{2+}$  into  $\text{Na}_{N-1}^+$  plus  $\text{Na}^+$  is to take a purely Coulombic approximation for the capture barrier  $B(d)$ :

$$B^{\text{Coulomb}}(d) = \frac{e^2}{d}, \quad (13)$$

where  $d$  is the distance between the centers of the two fragments. When  $d \simeq R(\text{Na}_{N-1}^+) + R(\text{Na}^+)$ , that is, close to the sum of the radii of the two fragments, Eq. (13) may not be a good approximation because of the penetration of the spilled-out electron density of the large fragment into the small one.

To obtain a better description of the fission barrier, we have used a deformed, self-consistent extended Thomas-Fermi model. We have considered as initial configuration (see top left panel of Fig. 2) that of a deformed cluster formed by two tangent jellium spheres, corresponding to clusters sizes  $N-1$  and  $1$ , respectively. For this configuration  $d$  is the sum of the radii of these two spheres. The other configurations along the dissociation coordinate have been obtained by increasing the separation between the two jellium spheres.

For any given separation, including the initial one, the ground-state electron density and the ground-state energy of the system are obtained by minimizing the energy functional of Eq. (7). In this case, the Euler-Lagrange equation (12) is a partial differential equation that, due to the axial symmetry of the problem, can be solved in cylindrical coordinates  $(r, z)$ . To do so, we have employed the so-called imaginary-time-step method.<sup>20-22</sup> We have used a  $\Delta r = \Delta z = 2$  a.u. mesh size, i.e., four times greater than the  $\Delta r$  that we have used in the spherical calculations.<sup>19</sup> To make sure that the electron density is negligible at the mesh edge, we have carried out the calculation in a  $30 \times 60$  a.u.<sup>2</sup>  $(r, z)$  box. Technical details concerning

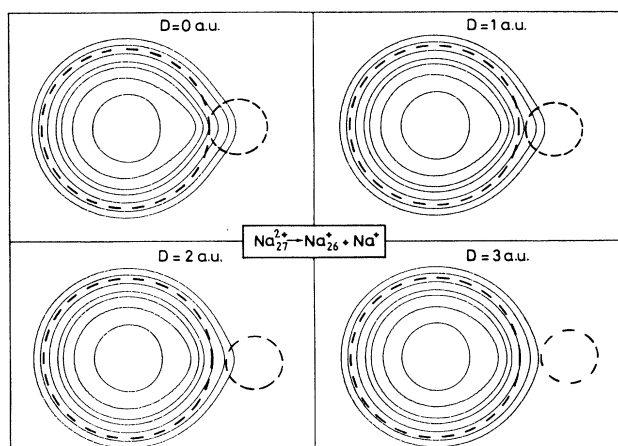
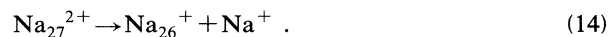


FIG. 2. Electron-density contour plots at four separations ( $D=0, 1, 2,$  and  $3$  a.u.) for the totally asymmetric fission channel of  $\text{Na}_{27}^{2+}$ .  $D$  is the separation between the jellium edges. The electron constant-density contour lines correspond, from outside to inside, to  $n=0.5 \times 10^{-3}, 1 \times 10^{-3}, 2 \times 10^{-3}, 3 \times 10^{-3}, 3.5 \times 10^{-3}, 4 \times 10^{-3}$  and again  $3.5 \times 10^{-3}$  a.u. The jellium edges are represented by dashed lines.

the spatial discretization of Eq. (12) and the obtainment of the direct Coulomb potential can be found in Refs. 23 and 24.

We have tested the two-dimensional ETF code by performing some spherical calculations with it. We have checked that the deformed code is able to reproduce the total energy of the  $\text{Na}_N^{2+}$  clusters obtained with the essentially exact spherical code to better than 0.5–1%. It takes less than 100 iterations of the two-dimensional code to stabilize the total energy of a given cluster within  $10^{-4}$  a.u.

Figure 2 shows electron-density contour plots at four separations along the reaction path for the totally asymmetric fission of  $\text{Na}_{27}^{2+}$ :



In this figure the separations, measured by the distance  $D$  between the sharp surfaces of the jellium spheres, are  $D=0, 1, 2,$  and  $3$  a.u. The edges of the jellium spheres are represented by dashed lines and the electron density by the solid line contours. The electron density plotted in each case is the one that minimizes the total energy for the corresponding cluster configuration. The electron constant-density contour lines correspond, from outside to inside, to  $n=0.5 \times 10^{-3}, 1 \times 10^{-3}, 2 \times 10^{-3}, 3 \times 10^{-3}, 3.5 \times 10^{-3}, 4 \times 10^{-3}$  and again  $3.5 \times 10^{-3}$  a.u. Notice that the density at the center of  $\text{Na}_{26}^{+}$  does not correspond to the maximum value due to the density oscillations at the jellium surface, clearly visible in all spherical ETF calculations (see, for instance, Ref. 19). The figure shows the appreciable polarization of the electron density of  $\text{Na}_{N-1}^{+}$  due to the presence of the  $\text{Na}^{+}$  ion. The polarization has a sizable effect on the height and shape of the fission barrier. The calculation correctly yields that, as the separation increases, the excess positive charge is

shared between the two clusters, i.e., the final products are singly charged.

Figures 3–5 show the shape of the capture barrier for the three cases  $\text{Na}_{20}^{2+}, \text{Na}_{27}^{2+},$  and  $\text{Na}_{40}^{2+}$ . The pure Coulomb barrier of Eq. (13) (dashed line) and the self-consistent ETF barrier (thick solid line) are shown as a function of the distance  $d$  between the centers of the two fragments, starting from an initial configuration in which the two positive jellium spheres are tangent. As is customary in similar problems, like that of nuclear  $\alpha$  disintegration,<sup>25</sup> the energies are referred to the value of the  $\text{Na}_{N-1}^{+} + \text{Na}^{+}$  system at infinite separation—that is,  $B(d)$  goes to zero when the distance  $d$  goes to infinity. The ground-state energy of  $\text{Na}_N^{2+}$  is indicated in each case by a horizontal line on the left part of each figure. The height of the fission barrier is then the difference between the top of the capture barrier and the horizontal line representing the ground-state energy of  $\text{Na}_N^{2+}$ .

The results of Figs. 3–5 show that, for large separation between the fragments, the barrier is purely Coulombic. However, the differences between the ETF and pure Coulombic barriers, due to spilled-out electron density in the ETF model, become evident for the relevant separations around the maximum of the ETF barrier. This difference, nevertheless, becomes rather small as the size  $N$  increases.

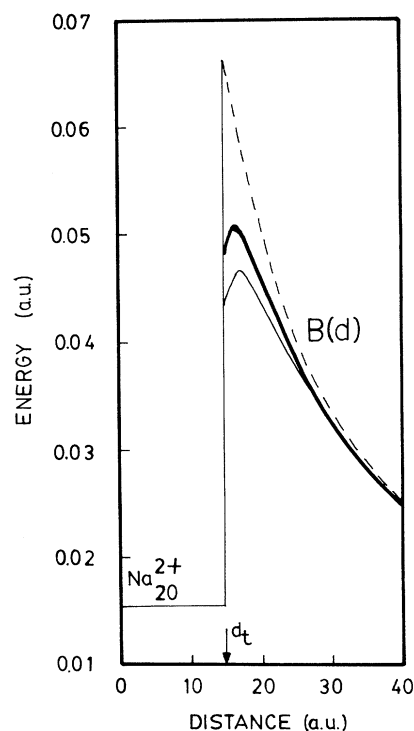


FIG. 3. Calculated capture barrier  $B(d)$  for the reaction  $\text{Na}_{19}^{+} + \text{Na}^{+} \rightarrow \text{Na}_{20}^{2+}$ . Dashed line, pure Coulomb approximation; thick solid line, extended Thomas-Fermi barrier; thin solid line, classical conducting-sphere model. Notice that the fission barrier  $F(d)$  is obtained by measuring  $B(d)$  from the ground-state energy of  $\text{Na}_{20}^{2+}$  [see Eq. (5)] which is indicated by a horizontal line on the left.

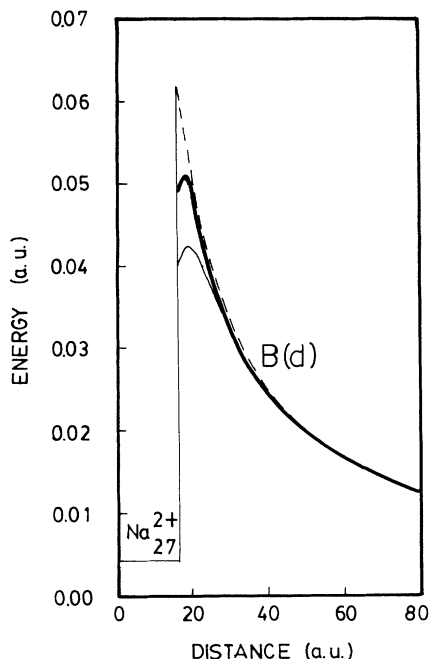


FIG. 4. Calculated capture barrier for the reaction  $\text{Na}_{26}^{2+} + \text{Na}^+ \rightarrow \text{Na}_{27}^{2+}$ . The meaning of the different lines and symbols is as in Fig. 3.

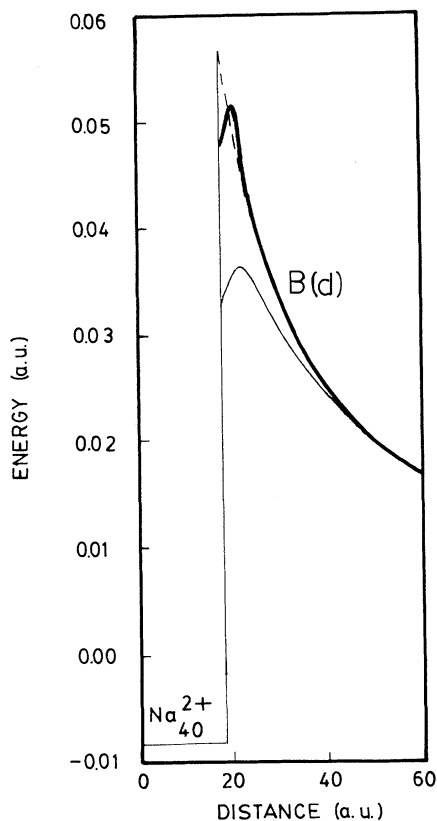


FIG. 5. Calculated capture barrier for the reaction  $\text{Na}_{39}^{2+} + \text{Na}^+ \rightarrow \text{Na}_{40}^{2+}$ . The meaning of the different lines and symbols is as in Fig. 3.

### C. Conducting-sphere model for the fission barrier

In this section we wish to consider the classical problem of an isolated conducting sphere (representing a cluster  $\text{Na}_{N-1}^{Q+}$ ) with net charge  $Q$  in the presence of a point charge  $q$ . The force acting on the charge  $q$  can be written from Coulomb's law:<sup>26</sup>

$$\mathbf{f} = \frac{q}{d^2} \left[ Q - \frac{qR^3(2d^2 - R^2)}{d(d^2 - R^2)^2} \right] \frac{\mathbf{d}}{d}, \quad (15)$$

where  $R$  is the radius of the conducting sphere and  $\mathbf{d}$  is the vector position of the charge  $q$  with respect to the center of the sphere. In the limit  $d \gg R$ , the force reduces to the usual Coulomb's law for two small bodies. But close to the sphere the force is modified because of the induced-charge distribution on the surface of the sphere.

From (15) we can compute the work made against the Coulomb forces when moving the charge  $q$  from infinite distance to a distance  $d$  from the center of the sphere:

$$B^{\text{classical}}(d) = \frac{qQ}{d} - \frac{q^2 R^3}{2d^2(d^2 - R^2)}. \quad (16)$$

From this equation we have computed the classical barrier, represented in Figs. 3–5 with a thin solid line. To be consistent with the other calculations,  $B^{\text{classical}}(d)$  has been plotted only for  $d \geq d_t$ , where  $d_t$  is the distance at which the two jellium spheres considered in Sec. II B above are tangent. The second term on the right-hand side (r.h.s.) of Eq. (16) accounts for the polarization of  $\text{Na}_{N-1}^+$  as  $\text{Na}^+$  approaches it coming from infinity. This polarization effect cancels part of the Coulomb repulsion and, consequently,  $B^{\text{classical}}(d)$  is below  $B^{\text{Coulomb}}(d)$  in the figures. Also, as a consequence of the polarization of the large cluster,  $B^{\text{classical}}$  has a maximum. This maximum occurs at a value of  $d$  very close to the corresponding maximum in  $B^{\text{ETF}}$ . Actually, the polarization of  $\text{Na}_{N-1}^+$  is also the reason for the maximum in  $B^{\text{ETF}}(d)$ . The maximum of  $B^{\text{classical}}$  is, however, smaller. This indicates that the classical model exaggerates the polarization effect. In the classical model an accumulation of negative charge is built on the surface region facing the approaching  $\text{Na}^+$  ion, and a deficit of charge appears on the opposite side of the cluster surface. However, the more realistic ETF calculations indicate that the charge deficit occurs in the interior of the cluster. The influence on the barrier height of this unrealistic feature of the conducting-sphere model increases with the radius  $R$ , as Figs. 3–5 show.

### III. DISCUSSION

Table I gives the ETF values of  $B_m$ ,  $\Delta H_f$ , and their sum  $F_m$  for four clusters investigated ( $N=10, 20, 27$ , and  $40$ ). In this range,  $B_m$  is remarkably constant, with a value close to 0.051 a.u. The value of  $\Delta H_f$  decreases fast for decreasing size of  $\text{Na}_N^{2+}$  and it changes sign (it becomes negative) at  $N=31$  (see also Ref. 4). As a consequence, the height of the fission barrier,  $F_m$ , also decreases fast for decreasing  $N$ . Our calculated  $F_m$  at

TABLE I. Calculated fission-barrier height ( $F_m$ ) and separated components ( $B_m$  and heat of reaction  $\Delta H_f$ ) for several  $\text{Na}_N^{2+}$  clusters. The heat of evaporation of a neutral monomer,  $\Delta H_e$  is also given. All quantities are in atomic units (1 a.u.=27.21 eV).

$N$	$B_m$	$\Delta H_f$	$F_m$	$\Delta H_e$
10	0.0515	-0.0460	0.0055	
20	0.0506	-0.0155	0.0351	0.0584
27	0.0510	-0.0044	0.0466	0.0596
31		-0.0004		0.0602
40	0.0516	0.0082	0.0598	0.0609
100		0.0324		0.0639

$N=27$  is 1.27 eV, in reasonable agreement with the value of 0.8 eV estimated by Bréchnignac *et al.*<sup>11</sup> A plot of  $F_m$  versus  $N$  indicates that the fission barrier vanishes for  $N=9$ . For this size and below, the doubly charged cluster spontaneously decays according to reaction (1). The heat of the evaporation reaction  $\Delta H_e$  is also given in Table I and plotted in Fig. 6.  $\Delta H_e$  is almost constant. Comparing the magnitudes of the fission barrier and  $\Delta H_e$  in Fig. 6, we observe that  $\Delta H_e$  is smaller than the fission barrier at large  $N$  and larger than it at low  $N$ . This is in agreement with the analysis of the experimental results of Bréchnignac *et al.*<sup>11</sup> and Saunders.<sup>13</sup> The crossing between the two curves occurs at  $N=41$ . This number is to be compared with the critical number  $N_c=27$  measured by Bréchnignac.<sup>11</sup> Our calculations overestimate  $N_c$ . This is not surprising considering the approximations made (jellium model, approximate kinetic-energy functional; see also further comments below). We stress, nevertheless, that the physics behind the existence of  $N_c$  is well reproduced by our calculations.

Our results then suggest the following interpretation of the so-called critical numbers for Coulomb explosion of

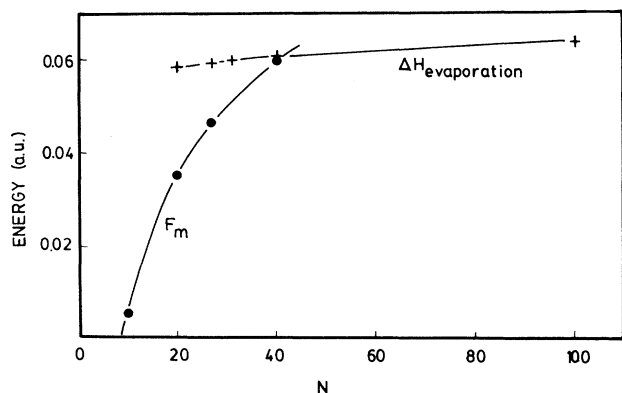


FIG. 6. Fission-barrier height ( $F_m$ ) vs cluster size  $N$ . Only the points for  $N=10, 20, 27$ , and  $40$  correspond to actual calculations and the line through them is only intended to guide the eye. The heat  $\Delta H_e$  for neutral-monomer evaporation is also plotted.

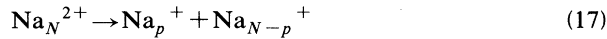
doubly charged clusters: We can define a critical number  $N_c$  (in our case,  $N_c=41$ ) such that fission is the preferred decay mode of excited clusters for  $N < N_c$  because the fission barrier is smaller than  $\Delta H_e$ . On the other hand, evaporation of a neutral atom competes with fission above  $N_c$ . This critical number, as indicated by Bréchnignac *et al.*,<sup>11</sup> should be observable when doubly charged clusters are formed by neutral monomer evaporation from hot clusters of higher masses. The results of our calculations suggest, however, a picture different from the one used until now<sup>11</sup> for the process of monomer evaporation.

When the distance  $d$  between the two fragments is still small, we can consider the system as a supermolecule. As such, what we have calculated and plotted in Figs. 3–5 is the minimum-energy curve of the supermolecule as a function of  $d$ . This implies that the barrier exists always (for a doubly charged cluster, we stress) and it must be overcome during the dissociation process, irrespective of the charge state of the small fragment after dissociation ( $\text{Na}^+$  or  $\text{Na}$ ). In other words, there is no way to avoid surpassing the fission barrier even for neutral-monomer evaporation. We then suggest that, after passing the barrier and when the system is undergoing dissociation, impelled by the Coulomb repulsion between the singly-charged fragments, the state  $\text{Na}_{N-1}^{2+} + \text{Na}$  appears suddenly as an available channel [see Fig. 1(right panel)]. This state can be realized when one electron of the supermolecule suddenly becomes localized around  $\text{Na}^+$ . For this to occur,  $d$  must still be small enough for the electron distribution of  $\text{Na}_{N-1}^+$  to overlap with that of  $\text{Na}^+$ . Since at the same time the two fragments are moving away from each other, a neutral  $\text{Na}$  atom can then escape. The probability for the dissociating supermolecule to choose the evaporation channel should increase as the energy difference  $\Delta V_{\text{IP}}$  between the two dissociated states ( $\text{Na}_{N-1}^+ + \text{Na}^+$  and  $\text{Na}_{N-1}^{2+} + \text{Na}$ ) decreases—that is, as  $N$  increases. This is supported by Saunders's experiments<sup>13</sup> on the dissociation of  $\text{Au}_N^{2+}$ . Notice that  $\Delta V_{\text{IP}}$  is just the difference between the second ionization potential of  $\text{Na}_{N-1}$  and the first ionization potential of neutral  $\text{Na}$ . Elucidating the details of the evaporation mechanism proposed here is beyond the capabilities of the present static-barrier calculations.

There is, on the other hand, a size range—in our case between  $10 \leq N \leq 40$ —where metastable doubly charged  $\text{Na}$  clusters may be observable if prepared by successive ionization of cold neutral clusters, under the condition that the doubly ionized cluster is left with an internal excitation energy below the top of the fission barrier.<sup>27</sup> Then we could define a second critical number  $N_c^*$  (in our case,  $N_c^*=9$ ), such that  $\text{Na}_N^{2+}$  is unstable for  $N \leq N_c^*$  because there is no fission barrier. It is likely that this picture also holds for other alkali-metal clusters but one should be careful in extrapolating it to other groups. For instance, according to the calculations by Reuse *et al.*,<sup>12</sup> the fission barrier does not vanish for low  $N$  in  $\text{Mg}_N^{2+}$ .

To put our results in a proper perspective, we stress that our model calculations have concentrated on the most asymmetric fission reaction—that is, the emission of

a charged monomer. But, in principle, the whole range of possibilities, represented by the different values of  $p$  in the reaction



should be investigated. If we focus on the heat of reaction  $\Delta H_f(p)$ , our ETF model predicts that  $p=1$  is the most favorable channel. However, other fission channels may lead to a more negative  $\Delta H_f$  if electronic shell-closing effects<sup>28</sup> are taken into account; these are absent in our simple ETF calculations. Additionally, as stressed in the discussion of our results above, the preferred fission channel is controlled by the height of the fission barrier and not by the size of  $\Delta H_f$ . In fact, channels with  $p \neq 1$  are sometimes dominant: for example, emission of  $\text{Au}_3^+$  in Saunders's experiments on  $\text{Au}_N^{2+}$  clusters.<sup>13</sup> So, a complete study of the fission barrier as a function of  $p$  should be performed for a complete understanding of the fission process. We plan to undertake this study in the near future. A preliminary investigation based on the purely Coulombic barrier of Eq. (13) leads to the following results:  $B_m^{\text{Coulomb}}$  is smaller for the emission of  $\text{Na}_2^+$  compared with the emission of  $\text{Na}^+$ ; on the other hand, the heat of the reaction (17) is more positive (less negative) for the emission of  $\text{Na}_2^+$ . Adding these two quantities, we find that the fission-barrier height is smaller for  $p=1$ , that is, for  $\text{Na}^+$ . These results should, however, be checked by a full ETF calculation of  $F(d)$ .

A further ingredient of the calculation that should be discussed is the value of the coefficient  $\lambda$  in the gradient term of Eq. (8). We have argued elsewhere<sup>29</sup> that the original von Weizsäcker value<sup>30</sup> ( $\lambda=1$ ) is the correct one for a good description of the electron density in the tail region of a finite system (atom, molecule, or cluster). However, from an empirical point of view, a value of  $\lambda=0.5$  has sometimes been found appropriate.<sup>19,31</sup> We have performed only a few exploratory calculations using  $\lambda=0.5$ . In the case of emission of  $\text{Na}^+$  from  $\text{Na}_{20}^{2+}$ ,  $B_m$  is almost identical to that given in Table I, which was calculated with  $\lambda=1$ . We then expect to find the same situation for other values of  $N$ . With respect to the heats of reaction, however, we have found some differences. As a general trend,  $\Delta H_f$  ( $\lambda=0.5$ ) is a little more positive than  $\Delta H_f$  ( $\lambda=1$ ), and it changes from negative to positive at  $N=23$  as  $N$  increases. This number is smaller than the

corresponding one ( $N=31$ ) for  $\lambda=1$ . But we expect the changes of the heat of evaporation to be similar to those in  $\Delta H_f$  and, consequently, a very small net effect when comparing the fission and evaporation channels.

#### IV. SUMMARY

In this paper we have used an extended Thomas-Fermi method and the jellium model to calculate the fission barrier for the emission of a  $\text{Na}^+$  ion from a doubly charged sodium cluster. The height of this barrier decreases as the size  $N$  of the parent cluster decreases and it vanishes in our model for  $N=9$ . Simple descriptions of the fission barrier which neglect the spill-out of the electron density give correctly the order of magnitude, although these are not accurate enough (as compared with the ETF barrier) in the region of the maximum of the barrier. In making this statement, one should keep in mind that the theory used to calculate the ETF barrier contains itself some approximate ingredients. We have also compared the barrier height to the energy needed to evaporate a neutral monomer. Neutral-monomer evaporation is the predicted preferred decay channel for hot clusters with large  $N$  whereas fission takes over for small  $N$ . This agrees with the experimental results of Bréchnignac *et al.*<sup>11</sup> and Saunders.<sup>13</sup> The transition between these two decay modes occurs at  $N_c=41$ . This number is not far from that deduced from the experiments of Bréchnignac and collaborators considering the approximations introduced in our model.<sup>32</sup> Between  $N=10$  and  $N=40$ , metastable doubly charged clusters may be observable if careful ionization from cold neutral clusters leaves the charged cluster with an energy below the barrier maximum.

#### ACKNOWLEDGMENTS

This work has been supported by Dirección General de Investigación Científica y Tecnológica (Grants PB 86-0654-C02 and PB 89-0332). The authors are grateful to A. Mañanes, L. C. Balbás, A. Rubio, and L. Serra for useful comments. One of us (J.A.A.) acknowledges the hospitality of the School of Physics, University of East Anglia.

\*Permanent address: Departament de Física, Universitat de les Illes Balears, E-07071 Palma de Mallorca, Spain.

<sup>1</sup>O. Echt, in *Physics and Chemistry of Small Clusters*, edited by P. Jena, B. K. Rao, and S. N. Khanna (Plenum, New York, 1987), p. 623.

<sup>2</sup>D. Tomanek, S. Mukerjee, and K. H. Bennemann, *Phys. Rev. B* **28**, 665 (1983).

<sup>3</sup>B. K. Rao, P. Jena, M. Manninen, and R. M. Nieminen, *Phys. Rev. Lett.* **58**, 1188 (1987).

<sup>4</sup>C. Baladrón, J. M. López, M. P. Iñiguez, and J. A. Alonso, *Z. Phys. D* **11**, 323 (1989).

<sup>5</sup>T. Jentsch, W. Drachsel, and J. Block, *Chem. Phys. Lett.* **93**, 144 (1983).

<sup>6</sup>C. Bréchnignac, M. Broyer, P. Cahuzac, G. Delacretaz, P. Labastie, and L. Wöste, *Chem. Phys. Lett.* **118**, 174 (1985).

<sup>7</sup>T. T. Tsong, *Surf. Sci.* **177**, 593 (1986).

<sup>8</sup>W. Schulze, B. Winter, and I. Goldenfeld, *Phys. Rev. B* **37**, 12937 (1988).

<sup>9</sup>F. Liu, M. R. Press, S. N. Khanna, and P. Jena, *Phys. Rev. Lett.* **59**, 2562 (1987).

<sup>10</sup>C. Bréchnignac, P. Cahuzac, F. Carlier, and J. Leygnier, *Phys. Rev. Lett.* **63**, 1368 (1989).

<sup>11</sup>C. Bréchnignac, P. Cahuzac, F. Carlier, and M. de Frutos, *Phys. Rev. Lett.* **64**, 2893 (1990).

<sup>12</sup>F. Reuse, S. N. Khanna, V. de Coulon, and J. Buttet, *Phys. Rev. B* **41**, 11743 (1990).

- <sup>13</sup>W. A. Saunders, *Phys. Rev. Lett.* **64**, 3046 (1990).
- <sup>14</sup>P. Joyes and P. Sudraud, *Surf. Sci.* **156**, 451 (1985).
- <sup>15</sup>N. Bohr and J. A. Wheeler, *Phys. Rev.* **56**, 426 (1939).
- <sup>16</sup>For a review, see *Theory of the Inhomogeneous Electron Gas*, edited by N. H. March and S. Lundqvist (Plenum, New York, 1983).
- <sup>17</sup>W. A. de Heer, W. D. Knight, M. Y. Chou, and M. L. Cohen, in *Solid State Physics*, edited by H. Ehrenreich, F. Seitz, and D. Turnbull (Academic, New York, 1987), Vol. 40, p. 93.
- <sup>18</sup>E. P. Wigner, *Phys. Rev.* **46**, 1002 (1934); *Trans. Faraday Soc.* **34**, 6781 (1938).
- <sup>19</sup>L. Serra, F. Garcias, M. Barranco, J. Navarro, L. C. Balbás, and A. Mañanes, *Phys. Rev. B* **39**, 8247 (1989).
- <sup>20</sup>D. Dalili, J. Nemeth and C. Ngô, *Z. Phys. A* **321**, 335 (1985).
- <sup>21</sup>F. Garcias, M. Barranco, J. Nemeth, C. Ngô, and X. Viñas, *Nucl. Phys. A* **495**, 169c (1989).
- <sup>22</sup>M. Centelles, M. Pi, X. Viñas, F. Garcias, and M. Barranco, *Nucl. Phys. A* **510**, 397 (1990).
- <sup>23</sup>H. Flocard, S. E. Koonin, and M. S. Weiss, *Phys. Rev. C* **17**, 1682 (1978).
- <sup>24</sup>K. T. R. Davies and S. E. Koonin, *Phys. Rev. C* **23**, 2042 (1981).
- <sup>25</sup>M. A. Preston and R. K. Bhaduri, *Structure of the Nucleus* (Addison-Wesley, Reading, MA, 1975), Chap. 11.
- <sup>26</sup>J. D. Jackson, *Classical Electrodynamics* (Wiley, New York, 1962), Chap. 2.
- <sup>27</sup>It is a trivial matter, already discussed by Liu *et al.* (Ref. 9) that the transmission coefficient for ion tunneling through the barrier is so small (due to the high effective mass of the particle) that the metastable doubly charged clusters with excitation energies below  $F_m$  can, for all practical purposes, be considered as “stable” clusters. We have verified, using the WKB approximation, that this is the case even for  $\text{Na}_{10}^{2+}$  which is the cluster with the smallest barrier.
- <sup>28</sup>M. P. Iñiguez, J. A. Alonso, M. A. Aller, and L. C. Balbás, *Phys. Rev. B* **34**, 2152 (1986).
- <sup>29</sup>J. A. Alonso and L. C. Balbás, *Structure and Bonding* (Springer-Verlag, Berlin, 1987), Vol. 66, p. 41.
- <sup>30</sup>C. F. von Weizsäcker, *Z. Phys.* **96**, 431 (1935).
- <sup>31</sup>L. Serra, F. Garcias, M. Barranco, J. Navarro, L. C. Balbás, A. Rubio, and A. Mañanes, *J. Phys. Condens. Matter* **1**, 10391 (1989).
- <sup>32</sup>We can expect the experimental critical number to be smaller than the theoretical one if the parent clusters have excitation energies exceeding the fission barrier.